

A NOVEL CARBON FIBER BASED POROUS CARBON MONOLITH

T. D. Burchell, J. W. Klett, and C. E. Weaver

INTRODUCTION

A novel porous carbon material based on carbon fibers has been developed. The material, when activated, develops a significant micro- or mesopore volume dependent upon the carbon fiber type utilized (isotropic pitch or polyacrylonitrile). The materials will find applications in the field of fluid separations or as a catalyst support. Here, the manufacture and characterization of our porous carbon monoliths are described.

A novel adsorbent carbon composite material has been developed^{1,2} comprising carbon fibers and a binder. The material, called carbon fiber composite molecular sieve (CFCMS), was developed through a joint research program between Oak Ridge National Laboratory (ORNL) and the University of Kentucky, Center for Applied Energy Research (UKCAER).

The materials are manufactured from milled carbon fibers and powdered phenolic resin, which are slurried in water and vacuum molded. The molding process allows the manufacture of slabs, tubes or more complex geometries with contoured surfaces. The "green" (as molded) artifact is heated at 130°C to cure the phenolic resin and then carbonized at 650°C. The resultant monoliths have bulk densities in the range 0.2 - 0.4 g/cm³ and crush strength of 1 - 2 MPa. Two carbon fiber types have been utilized in our work to date. First, petroleum-pitch derived isotropic carbon fibers have been fabricated into monoliths and activated in steam or CO₂ at 850°C. The material develops significant microporosity, with mean pore sizes in the range 0.5 - 1.0 nm, and micropore volumes in the range 0.2 - 0.5 cm³/g. Second, monoliths have been manufactured from polyacrylonitrile (PAN) derived carbon fibers. These materials develop significant mesoporosity in the size range 2-50 nm and mesopore volumes typically exceeding 0.5 cm³/g, making them potential catalyst support materials. In both cases the composites are strong and porous, allowing fluids to easily flow through the material.

The isotropic pitch derived carbon fiber porous carbon monolith, when activated, provides a high micropore surface area (> 1900 m²/g) capable of rapid adsorption and desorption. The activated fiber micropore distribution is very narrow, with mean micropore sizes < 1 nm, allowing molecular

sieving on the basis of molecular size and shape. A potentially large application for our carbon-fiber based porous monoliths is gas separation using the Pressure Swing Adsorption (PSA) process.

Separation by adsorption is based on the selective accumulation of one or more components of a gas mixture on the surface of a microporous solid. When a gaseous mixture is exposed to an adsorbent for sufficient time, an equilibrium is established between the adsorbed phase and the gas phase. The gas phase becomes richer in the less selectively adsorbed component. The attractive forces responsible for adsorption are of the Van der Waals type. Desorption can be achieved either by increasing the temperature of the system or by reducing the adsorbate pressure. The desorption step also regenerates the adsorbent surface for reuse during the subsequent adsorption step. Thus, the adsorptive separation process consists of a cyclic sequence of adsorption and desorption steps. When desorption is achieved by decreasing the pressure, the process is called pressure swing adsorption. One of the components of a gas mixture is selectively adsorbed at higher partial pressure and desorbed subsequently by lowering the partial pressure. The change in partial pressure of the component gas can be caused either by decreasing the total pressure, changing the composition of the gaseous mixture, or by a combination of both.

Here we report the synthesis and characterization of CFCMS material, particularly with respect to micropore and mesopore structure. Moreover, the results of CO₂ uptake studies on microporous monoliths are reported.

EXPERIMENTAL

Nitrogen adsorption isotherms were measured at 77 K using our Autosorb-1 instrument. Micropore size analysis used a variety of methods, including the Brunauer, Emmett and Teller³ (BET) method for surface area and the Dubinin-Redushkevich (DR) method for micropore volume and micropore size. Additional micropore size estimates were obtained using the Horvath-Kawazoe (HK) and Dubinin-Astakhov (DA) methods. Mesopore (2-50 nm) and macropore (>50 nm) size, area, and volume data were obtained using a Micromeritics Autopore II mercury intrusion apparatus. Intrusion measurements were performed over the pressure range vacuum (~10 μ m Hg) to 90,000 psia. Equilibration times of 10 and 60 seconds were used for the low and high pressure measurements, respectively. CFCMS materials were subjected to microstructural examination using an ISI SS40 scanning electron microscope (SEM). CO₂ uptake was measured using a Mettler thermal

microbalance. Specimens were thoroughly outgassed by heating them to 300°C under vacuum on the microbalance. The specimens were then cooled under vacuum to room temperature and the balance back-filled with CO₂. The weight loss and gain was measured when the specimen temperature was swung from 30 to 110°C and back to 30°C.

RESULTS AND DISCUSSION

CFCMS Synthesis

The CFCMS material was fabricated at ORNL using a process initially developed by the DOE for the production of thermal insulators for NASA space missions⁴. Carbon fibers derived from either isotropic petroleum pitch, or PAN, were mixed in a water slurry with powdered phenolic resin. The slurry was transferred to a molding tank and the water drawn through a porous mold under vacuum. The resulting green artifact was dried, cured in air at 60°C, and stripped from the mold. The composite was cured at ~150°C in air prior to carbonization at 650°C under an inert gas. The CFCMS synthesis route is illustrated in Fig. 1. A schematic diagram of the molding arrangement is shown in Fig. 2. The fabrication process allows the manufacture of slab or tubular forms. Moreover, we believe that it will be possible to mold contoured plates, and tubes, to near net shape via this synthesis route. Once carbonized, CFCMS is readily machined to more complex geometries. Typical carbonized bulk densities of our CFCMS materials are 0.3-0.4 g/cm³.

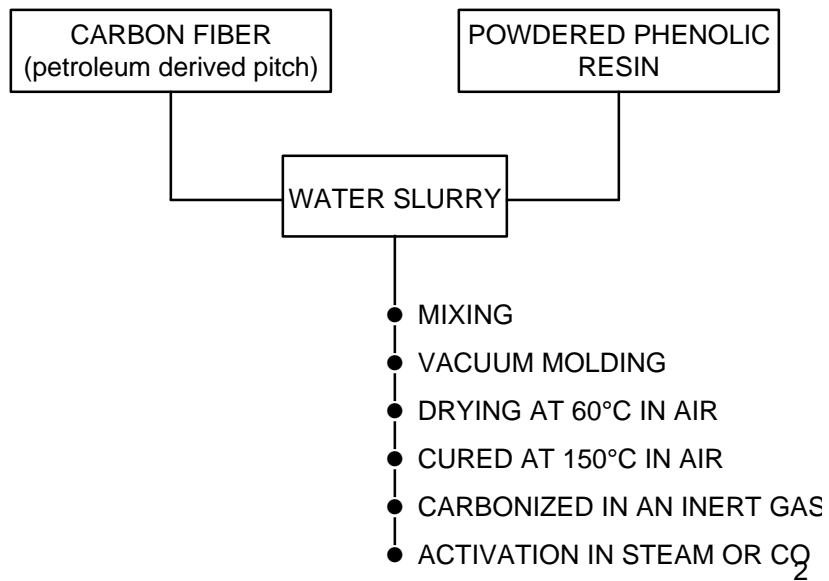


Fig. 1. CFCMS synthesis route.

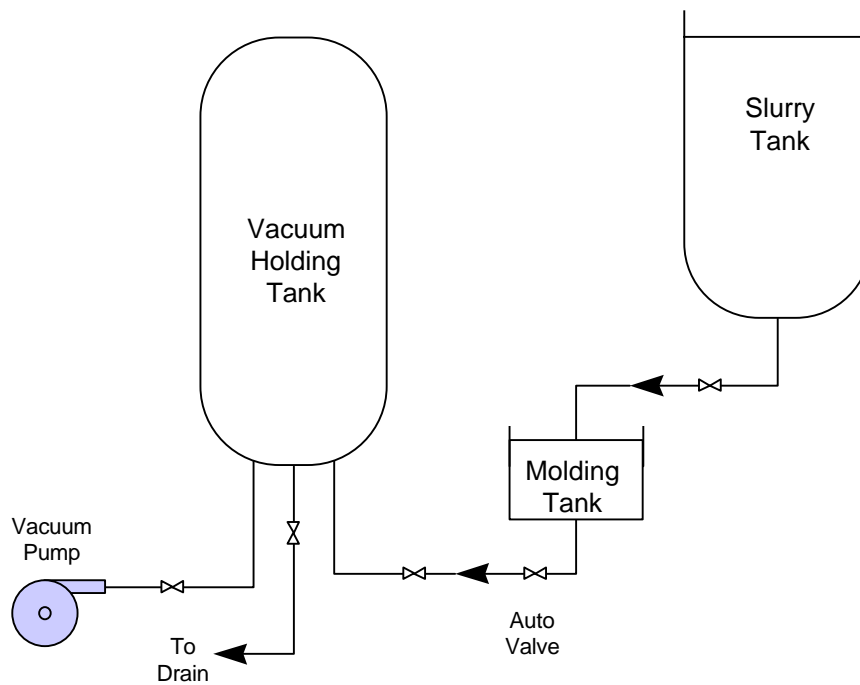


Fig. 2. Schematic illustration of the CFCMS molding apparatus.

Characterization

Microporous Carbon Fiber Monoliths

Figure 3 ($\times 200$ magnification) shows the structure of our CFCMS material manufactured from isotropic pitch derived carbon fibers. The chopped fibers are bonded at their contact points. The carbon fibers are approximately 10-20 μm diameter, whereas the macro-voids between the fibers are typically $>30 \mu\text{m}$ in size. The resultant open structure allows free flow of fluids through the material and ready access to the carbon fiber surface. Previously, we reported the carbon fiber length distribution.

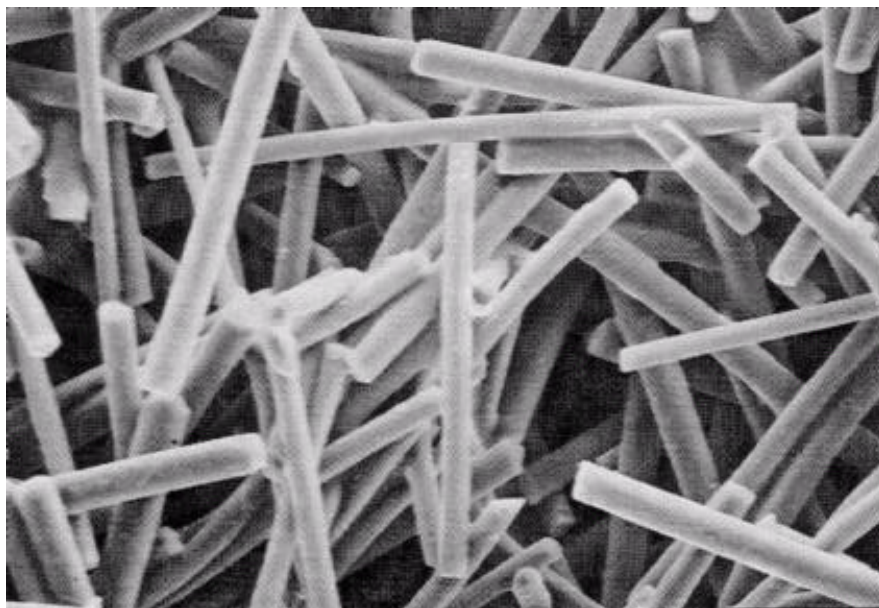


Fig. 3. SEM micrograph of carbon fiber composite molecular sieve (magnification $\times 200$).

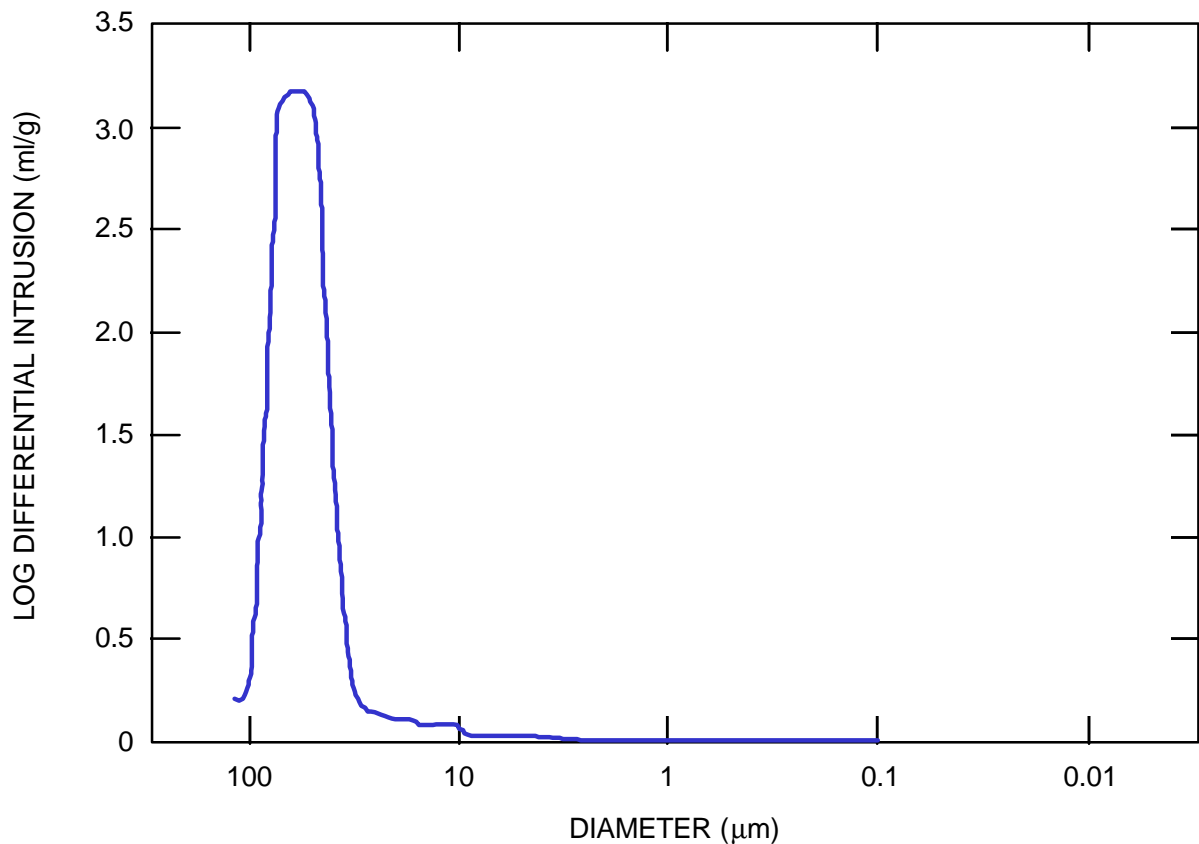


Fig. 4. CFCMS macropore size distribution for a pitch derived carbon fiber monolith obtained from mercury intrusion data.

The distribution mode is $\sim 400 \mu\text{m}$ and the fiber lengths are widely distributed and range from 100 to 1000 μm . Mercury porosimetry data for the CFCMS material in the unactivated condition are shown in Fig. 4, and indicate the macropore size range to be approximately 10-100 μm . The macropores are the voids between the fibers, and mercury porosimetry data for macropore sizes are in agreement with visual observations made from SEM images (Fig. 3).

A series of CFCMS materials were prepared at ORNL and activated at UKCAER. Details of the activation conditions are given in Table 1 along with the results of our analysis of the microporosity.

Table 1. Activation conditions and micropore characterization data.

Spec. Ident.	Activation Conditions				Micropore Analysis Data				
	Temp (°C)	Time (mins)	Agent	Burn-off (%)	BET Area (m ² /g)	Micropore Width (nm)			DR Pore Vol (cm ³ /g)
						HK	DA	DR	
160	800	30	H ₂ O	7	394	0.48	1.3	0.58	0.20
161A	950	10	CO ₂	6	292	0.48	1.8	1.21	0.13
161B	950	10	CO ₂	6	281	0.47	1.9	1.34	0.10
166	800	180	H ₂ O	17	762	0.48	1.48	0.75	0.39
167	800	360	H ₂ O	28	891	0.49	1.5	0.76	0.49
170	950	180	CO ₂	32	1132 1038	0.47	1.6	0.78 0.76	0.48
46	850	90	H ₂ O	28	1461	0.62	1.3	0.67	0.73

The BET surface areas reported in Table 1 ranged from 281 to 1461 m²/g, and the mean micropore size (DR method) varied from 0.58-1.34 nm. Moreover, the micropore volumes (DR method) varied from 0.1 - 0.73 cm³/g. The large surface area, combined with a large volume of micropores, suggests these materials might have a strong affinity for the adsorption of light gases. Therefore, CO₂ adsorption studies were performed, and our data are reported in Table 2.

Large CO₂ uptakes were measured for the CFCMS samples. As a comparison a commercial coconut shell carbon was evaluated, and was shown to have adsorbed ~20% less CO₂ than our best CFCMS. Moreover, the adsorption process was significantly slower in the case of the coconut shell carbon, where resorption of the CO₂ on cooling from the temperature swing took >2 hours compared with <1 hour for the CFCMS materials. The superior adsorption kinetics of the CFCMS are ascribed to the small diameter of the carbon fibers (10-20 μm) compared to the ~2-3 mm of the coconut shell carbon. The diffusion path for the CO₂ to an adsorption site is, therefore, substantially shorter in

Table 2. CO₂ uptake data and micropore data

Spec. Ident.	CO ₂ Uptake data				Micropore Analysis Data				
	Sample Mass (mg)	Wt% CO ₂ Uptake	Vol CO ₂ Ads. (cm ³)	Spec. CO ₂ Ads. Capacity (cm ³ /g)	BET Surf. Area (m ² /g)	Micropore Width (nm)			DR Pore Vol (cm ³ /g)
						HK	DA	DR	
160	89.50	7.8	3.95	44	394	0.48	1.3	0.58	0.20
161	72.45	6.9	2.53	35	292	0.48	1.8	1.21	0.13
166	89.95	8.9	4.05	45	762	0.48	1.5	0.75	0.39
167	92.27	8.7	4.04	44	891	0.49	1.5	0.76	0.49
170	74.89	10.3	3.9	52	1132	0.47	1.6	0.76	0.48
46	73.88	8.5	3.2	43	1461	0.62	1.3	0.67	0.73
Coconut shell carbon	90.22	8.3	3.8	42	168	0.5	1.6	-	-

the case of the CFCMS. The CO₂ adsorption capacity of CFCMS is clearly related to the BET surface area and micropore volume, as shown in Figs. 5 and 6, respectively. The weight percent of CO₂ adsorbed increases with increasing pore volume and BET surface area, apparently reaching peak adsorption capacity at micropore volumes of ~0.5 cm³/g and BET surface areas of ~1000 m²/g (e.g., sample 170). Figure 7 shows CO₂ uptake plotted as a function of micropore size (DR method). The optimum pore size appears to be ~0.8 nm. Significantly, samples 161 and 160 showed the lowest CO₂ uptakes (6.9 and 7.8% respectively), yet they possessed the largest and smallest mean micropore sizes (1.21 and 0.58 nm) respectively, suggesting a strong sensitivity of CO₂ uptake to the micropore size.

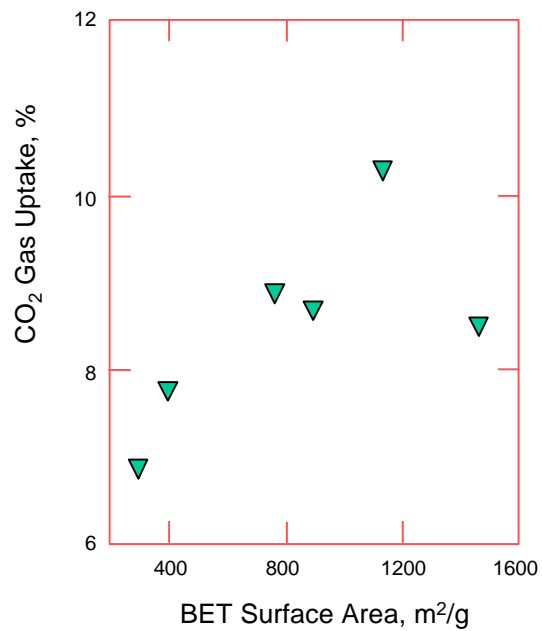


Fig. 5. The relationship between CO₂ uptake and BET surface area for CFCMS.

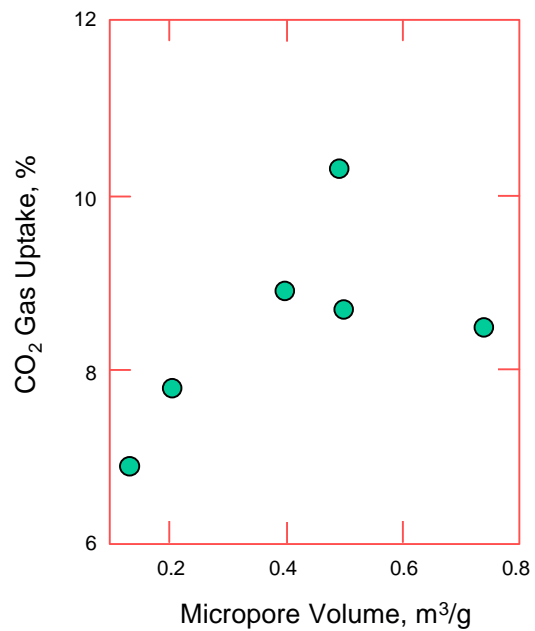


Fig. 6. The relationship between CO₂ uptake and micropore volume for CFCMS.

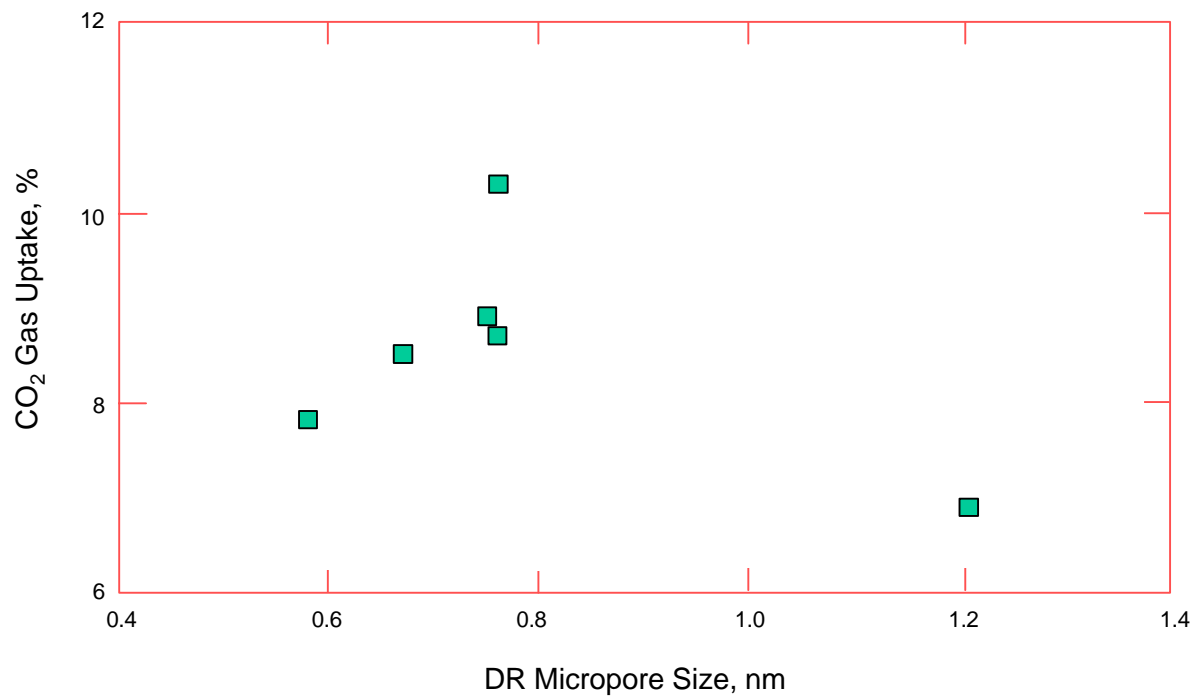


Fig. 7. The relationship between CO₂ uptake and mean micropore size for CFCMS.

Mesoporous Carbon Fiber Monoliths

A series of carbon fiber monoliths⁵ were prepared from PAN derived carbon fibers and activated to burn-offs (% weight loss on activation) up to ~22%. Subsequent characterization using mercury porosimetry revealed the material to be highly mesoporous. Figure 8 shows the cumulative mesopore surface area as a function of pore diameter. The surface area is clearly associated with pores of size <50nm, i.e., the mesopores. The carbonized monoliths exhibited surface areas >500 m²/g and mesopore volumes >1 cm³/g. In contrast, the as-received PAN fibers exhibited a mesopore volume of only 0.28 cm³/g. Evidently, the carbonization process radically affects the PAN fiber pore structure, possibly by opening the surface pores sufficiently to make the internal pores accessible. Access to the fiber's internal pore structure could occur when reactive species such as O₂, CO₂, H₂O and CO (which were adsorbed during monolith manufacture) are subsequently desorbed during carbonization and gasify the carbon.

The effect of steam activation on the mesopore volume is shown in Fig. 9. The mesopore volume was found to rapidly decrease with increasing burn-off, from >1 cm³/g at zero burn-off to <0.4 cm³/g at ~10% burn-off. Similarly, the mesopore surface area was found to decrease with

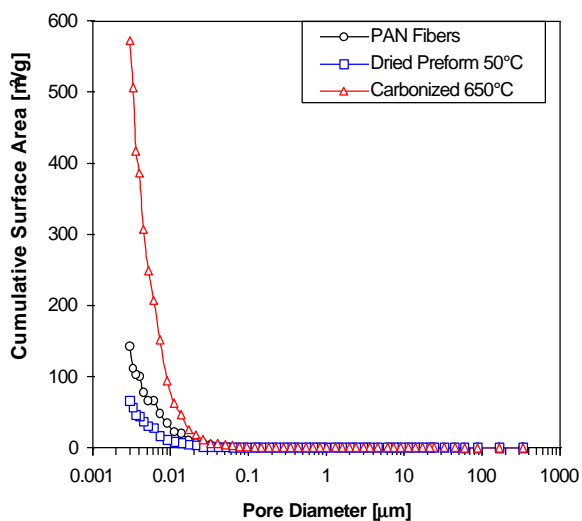


Fig. 8. Mesopore surface area as a function of pore diameter obtained from mercury intrusion data for our PAN derived carbon fiber porous carbon monoliths.

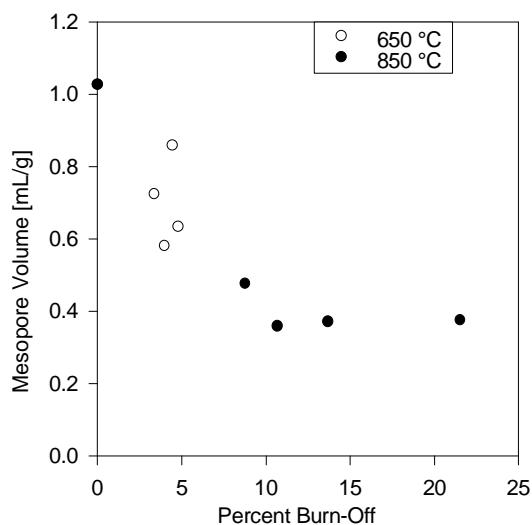


Fig. 9. Mesopore volume as a function of burn-off for our PAN derived carbon fiber porous monoliths.

increasing burn-off, falling from $>500 \text{ m}^2/\text{g}$ at zero burn-off to $<200 \text{ m}^2/\text{g}$ at $\sim 10\%$ burn-off (Fig. 10). The mean mesopore diameter is shown as a function of burn-off in Fig. 11. In the carbonized condition, the carbon fiber monoliths exhibited a mean mesopore width of $\sim 7.2 \text{ nm}$. Activation caused the mean mesopore size to increase, reaching $\sim 8.7 \text{ nm}$ at the peak burn-off considered here.

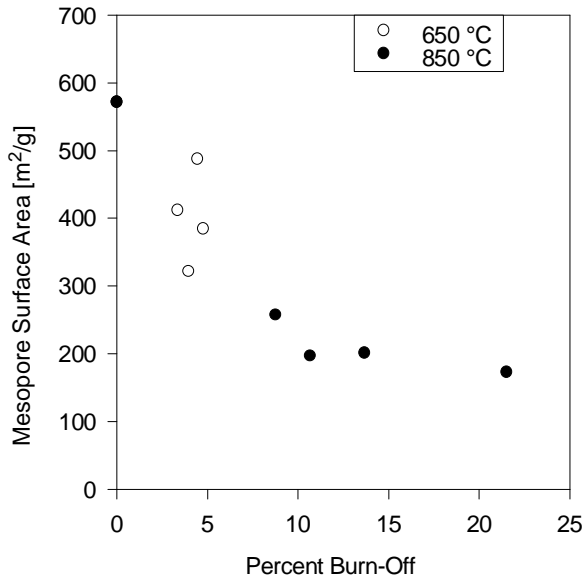


Fig. 10. Mesopore surface area as a function of burn-off for our PAN fiber derived porous carbon monoliths.

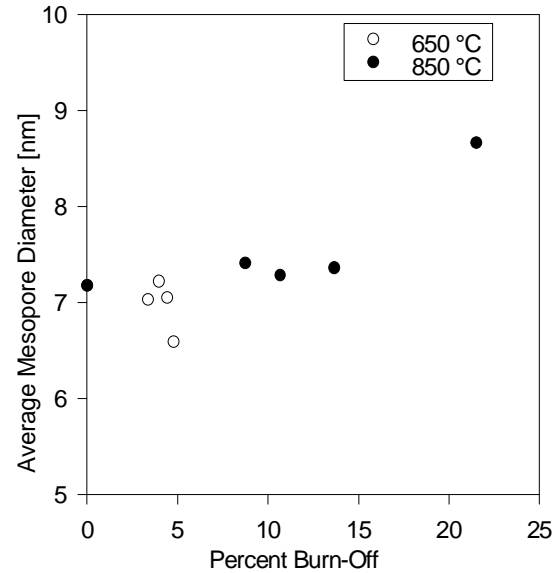


Fig. 11. Mean mesopore diameter as a function of burn-off for our PAN fiber porous carbon monoliths.

The large volume of mesopores observed in the PAN derived fiber monoliths is attributed to the fibril structure of PAN carbon fibers⁶. Typically⁷, the crystallite size in a PAN fiber is $\sim 1.6 \text{ nm}$. Moreover, there is extensive folding of the fibril nature of these crystallites, creating extensive pore networks in the mesopore size range, as confirmed by the data in Fig. 8. The modest increase of mesopore size with increasing burn-off (Fig. 11) suggests that the steam activation process effected very little change to the internal pore structure of the fiber. However, steam activation substantially reduced both the specific mesopore volume and associated specific mesopore surface area (Figs. 9 and 10). Moreover, SEM examination showed that the carbon fiber diameter reduced substantially during activation, indicating the fibers are consumed radially by a process of gasification of their external surface. The observed variations of pore size, pore volume, and surface area with burn-off could be readily explained if activation of the PAN carbon fibers occurred via a constant penetration depth,

moving-front reaction. In such a process the pore structure would first be developed by gasification of the pore walls, increasing the pore size and volume. With further burn-off, the fiber itself is consumed, thus destroying the pore structure. As the reaction front moves from the periphery of the fiber toward its core, reducing the fiber diameter, the total volume of pores being created or developed is reduced. The high mesopore volume in the carbonized monolith suggests that, in this instance, activation is not required. Significant reductions in process time, and a beneficial cost saving, may thus be realized.

CONCLUSIONS

A novel porous monolithic carbon fiber composite material, known as CFCMS, has been developed and shows considerable potential for use in PSA gas separation systems. The material can be fabricated in large sizes yet retains the advantageous gas adsorption and separation properties of its precursor isotropic pitch derived carbon fibers. The CFCMS material structure contains large voids ($>30\ \mu\text{m}$) between the $10\text{-}20\ \mu\text{m}$ diameter fibers which allows for free flow of fluids through the material. A series of microporous CFCMS materials have been prepared and characterized. Their CO_2 adsorption characteristics were examined and determined to be superior to a commercially available activated carbon. The CO_2 adsorption capacity of CFCMS materials is related to both the BET surface area and the micropore volume, and appears to be particularly sensitive to the mean micropore size.

Mesoporous CFCMS materials were prepared from PAN derived carbon fibers. The materials exhibited mesopore volumes in excess of $1\ \text{cm}^3/\text{g}$ and, therefore, are candidates for catalyst support applications. Steam activation of the monoliths increased the mean mesopore size only modestly, but reduced the mesopore volume and mesopore surface area significantly. The largest mesopore volumes were associated with the samples that had not been activated, but rather had only been carbonized. An activation and pore structure development mechanism was postulated to explain the pore characterization data obtained from mercury intrusion analysis.

ACKNOWLEDGEMENTS

Research sponsored by the U.S. Department of Energy, Office of Fossil Energy, Advanced Research and Technology Development Materials Program [DOE/FE AA 15 10 10 0, Work Breakdown Structure Element ORNL-1(E)] under contract DE-AC05-84OR21400 with Martin Marietta Energy Systems, Inc.

REFERENCES

1. T. D. Burchell, "Carbon Fiber Composite Molecular Sieves," in *Proc. Eighth Annual Fossil Energy Materials Conference*, Oak Ridge, Tennessee, May 10-12, 1994. CONF-9405143, ORNL/FMP-94/1, pp. 63-70, Pub. Oak Ridge National Lab., Aug. 1994.
2. Frank Derbyshire, "Activation and Micropore Structure Determination of Carbon Fiber Composite Molecular Sieves," in *Proc. Eighth Annual Fossil Energy Materials Conference*, Oak Ridge, Tennessee, May 10-12, 1994. CONF-9405143, ORNL/FMP-94/1, pp. 137-143, Pub. Oak Ridge National Lab., Aug. 1994.
3. S. Brunauer, P. H. Emmett, and E. Teller, *J. Am. Chem. Soc.*, Vol 60, p. 309 (1938).
4. George C. Wei and JM Robbins, "Carbon-Bonded Carbon Fiber Insulation for Radioisotope Space Power Systems," *Ceramic Bulletin*, Vol. 64, No. 5, p. 691 (1985).
5. J. W. Klett and T. D. Burchell, "Carbon Fiber Carbon Composites for Catalyst Supports," *Proc. 22nd Conf. on Carbon, San Diego, California, July 1992*, Pub. American Carbon Society.
6. R. J. Diefendorf and E. W. Tokarsky, *Polymer Eng. Sci.*, Vol. 15, P. 150 (1975).
7. J. P. Donnet and R. C. Bansal, *Carbon Fibers*, Pub. Marcel Dekker, Inc., New York (1990).